# Seismotectonics of Badra-Amarah Fault, Iraq-Iran Border

**Article** · June 2016

**4 authors:**

Wathiq Abdulnaby
University of Basrah
**16** PUBLICATIONS **82** CITATIONS

SEE PROFILE

Maher Mandeel Mahdi
University of Basrah
**19** PUBLICATIONS **43** CITATIONS

SEE PROFILE

Rafed Al-Mohmed
University of Basrah
**3** PUBLICATIONS **13** CITATIONS

SEE PROFILE

Hanan Mahdi
University of Arkansas at Little Rock
**40** PUBLICATIONS **375** CITATIONS

SEE PROFILE

Some of the authors of this publication are also working on these related projects:

both articles View project

Seismology View project

# Seismotectonics of Badra-Amarah Fault, Iraq-Iran Border

Wathiq Abdulnaby[1], Maher Mahdi[2], Rafed Al-Mohmed[3], Hanan H. Mahdi[4]

[1,2,3]*Seismological Lab of University of Basrah (SLUB) Department of Geology, College of Sciences, University of Basrah, Basrah, Iraq*
[4]*Graduate Institute of Technology (GIT) University of Arkansas at Little Rock (UALR), Arkansas, USA*

***Abstract:*** *Badra-Amarah fault is located in the northeastern side of the Mesopotamian Zone at the Iraq-Iran border. This fault is the most seismically active fault in Iraq and it is located within the seismic zone that could suffer a major damage. The goal of this study is to investigate the seismic history and the focal mechanism solutions of Badra-Amarah fault. Additionally, recent stress regime of the fault area was derived by conducting formal stress inversion technique. The seismic history has been studied by using the source parameters of earthquakes from different catalogs, mainly from the IRSC catalog. The focal mechanism solutions were assembled from the GCMT project, which were analyzed in this study to derive the principal stress directions and their regimes. According to the seismic history of the study area, four seismic swarms occurred along the fault in August, 2008, June, 2009, August, 2009, and April, 2012 with magnitude of mainshocks ranges from 4.4 to 5.7. The focal mechanism solutions show that Badra-Amarah fault has a reverse movement with little strike-slip displacement. The dip of the fault is 60° with dip direction equals 226°. From the stress inversion of focal mechanisms, the principal stress axes are: $\sigma_1$ is 14°/217°, $\sigma_2$ is 10°/309°, and $\sigma_3$ is 72°/074°. The length of fault is about 200 km and its depth may reach the basement rocks, which are about 10 km. The fault extends to the northwest to reach Mandali city.*

***Keywords:*** *Seismotectonics of Iraq, Mesopotamian Zone, Focal mechanism solutions, Stress analyses, Arabian plate, Badra-Amarah fault.*

## I. Introduction

Iraq represents part of the convergent plate boundary between the Arabian and Eurasian plates. The collision between these plates began after the closure of the Neo-Tethys Ocean in the Miocene and it continues to the present day (e.g. Dewey *et al*., 1973 and Numan, 1997). Iraq has two systems of faulting; these are the transversal faults and longitudinal faults (Najd system faults). One of the longitudinal faults is the Makhul-Hemrin fault. It trends from center of Iraq and passing through the Makhul and Hemrin folds until Badra and Amarah cities at the Iraq-Iran border (Jassim and Goff, 2006). In this study, the Makhul-Hemrin fault is suggested to be divided into two faults based on the seismicity and structural geology of the study area. These two faults are: the Makhul-Hemrin listric fault and Badra-Amarah fault (red broken line in figure 1). Listric fault is parallel to the Makhul and Hemrin fold axes and seems to be non-active fault. It forms the boundary between Folded and Unfolded Zones. Badra-Amarah fault extends from Badra to Amarah cities and it is seismically active. Seismic activity is extending only along the longitudinal area between Badra and Amarah cities. The Makhul-Hemrin listric fault has different direction than the direction of Badra-Amarah fault (Fig. 1).

The goal of this study is to investigate the seismic history, focal mechanism solutions, and recent stress analysis of Badra-Amarah fault. This goal can be achieved by using the source parameters and moment tensor solutions of earthquakes from different catalogs, such as the Iranian Seismological Center (IRSC), the European-Mediterranean Seismological Centre (EMSC), the Incorporated Research Institutions for Seismology (IRIS), and the Global Centroid-Moment-Tensor (GCMT) Project.

## II. Seismotectonic Setting

The Mesopotamian Zone is bounded by the NW-SE trending Euphrates fault in the southwest and the NW-SE trending Makhul-Hemrin fault in the northeast (Fig. 1). These two faults have surface expression represented by linear features and alluvial fans which borders the Mesopotamian Zone on both sides. The Euphrates fault was formed by the Najd Orogeny (Pre-Cambrian). It runs from the Rutba area in western Iraq and continues towards Basra in south. It forms the boundary between the Quaternary Mesopotamian Plain and the rocky desert of southwest Iraq. The fault was reactivated during Late Jurassic and Cretaceous time (Jassim and Goff, 2006). The Makhul-Hemrin fault extends along Iraq-Iran border in southeast Iraq. It forms the boundary between unfolded zone (the Mesopotamia) and folded zone. This fault was reactivated during the Pliocene and it is still active at present day (Jassim and Goff, 2006). The northern boundary of the Mesopotamian Zone is represented by one of the Makhul-Hemrin anticlinal chain. The Mesopotamian Zone extends to the Arabian Gulf in the southeast of the Arabian plate.
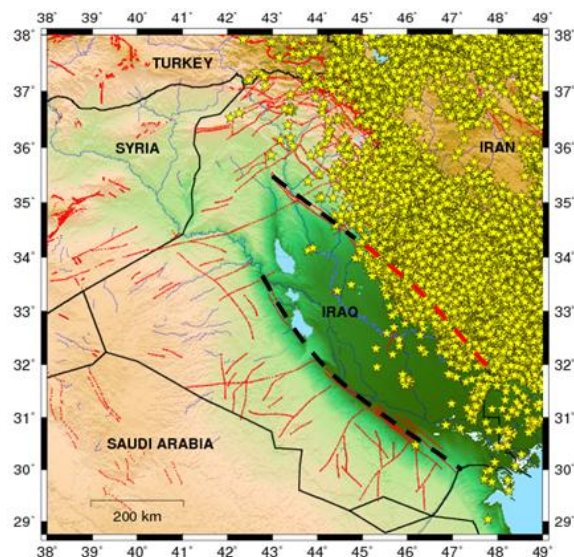
**Figure 1:** Seismicity of Iraq and adjacent areas taken from the IRSC (from 1/1/2006 to 1/10/2014) represented by yellow stars. The IRSC catalog ends at longitude 42°E. Broken black lines depict the Makhul-Hemrin fault in the northeast and the Euphrates fault in the southwest. Broken red line is Badra-Amarah fault.

According to Numan (1997), the Mesopotamian Zone is a sagged basin and represents a huge graben that formed as a result of subsidence of the block located between the Euphrates and Makhul-Hemrin faults during the extensional tectonic phase of the Mesozoic Era (Fig. 1). Alluvial fans on the eastern side of the Mesopotamia have developed along Badra-Amarah fault, which is the southern part of the Makhul-Hemrin fault as mentioned earlier, from Badra in the northwest to Amara in the southeast. Alluvial fans on the western side of the Mesopotamia are located along the Euphrates fault. Badra-Amarah fault represents the boundary between Mesopotamian Zone in Iraq and Dezful Embayment in Iran.

Studying the seismicity of Badra-Amarah fault is important because it represents the northeastern boundary of the Mesopotamian Zone, and this zone composes about 25% of the area of Iraq and subsists 60% of its population (Jassim and Goff, 2006). According to the isointensity map, the Mesopotamian Zone is located within the seismic zone of minor damage that follows intensities range from IV to V (MM magnitudes). On the other hand, Badra-Amarah fault is part of the seismic zone of major damage with intensity of VIII (MM magnitudes). Earthquakes in the Mesopotamian Zone cause damage due to liquefaction of the Quaternary sediments (Jassim and Goff, 2006). This should be of a major concern to the seismological community in Iraq, since the area is seismically active and has very thick alluvial sediments which should be susceptible to liquefaction due to earthquake shaking.

Figure 1 represents the seismic activities of Iraq and adjacent areas according to the (IRSC) catalogs. The IRSC catalog ends at longitude 42°E. This figure indicates that the seismic activity of Iraq is moderate to high at northern and northeastern parts, and decreases in the south and southwestern direction.

### III.    Seismic History of Badra-Amarah Fault

Identifying earthquake swarms is an important step before study the seismic history of the study area. Keilis-Borok *et al*. (1978) defined a swarm as 'spatial clustering of earthquakes at a time when the seismicity of the region is above average'. Based on this identification, a swarm must meet criteria in both time and space domains, which must be true simultaneously for a swarm to exist (Michael and Toksoz, 1982). Each swarm must have a mainshock, which is the largest earthquake in a sequence. The mainshock sometimes is preceded by one or more foreshocks, and almost always followed by many aftershocks.

According to the (IRSC) catalog, about 3074 earthquakes were recorded in the study area (latitude 31°N to 34°N and longitude 45°E to 42°E) for the time period from January 1st, 2006 to October 1st, 2014 (Fig. 2, left panel). For this period of time, four seismic swarms occurred along Badra-Amarah fault. Swarms one (yellow stars) and four (sky blue stars) occurred near the Amara city, while swarms two (green stars) and three (blue stars) occurred near the Badra city (Fig. 2, right panel). Table 1 shows the basic seismic parameters of the mainshocks of these four swarms taken from different catalogs.

The first swarm extends for 16 days from 27-08-2008 to 9-9-2008. The mainshock happened after three days of the foreshocks with magnitude 5.7, while the rest of days represent the aftershock. The fourth day of the swarm had 31 events which represents the largest number of earthquakes in the swarm. The second swarm lasted 10 days from 20-06-2009 to 30-06-2009. The mainshock happened at the fifth day of the swarm with

magnitude 4.5 and this day had the largest number of earthquakes. The third swarm represents the shorter swarm. It lasted 8 days from 27-08-2009 to 04-09-2009. The mainshock occurred on the third day. The fourth swarm lasted for 13 days started from 18-04-2012 to 30-04-2012. The mainshock happened after three days and represents the most frequent with rate of 54 events (Fig. 3).

The effects of earthquakes that occur at Badra-Amarah fault reach many cities in southern Iraq in the Mesopotamian Zone. Cities such as Badra, Amarah, Basra, Nasiriyah, and Kut were affected by the seismic activities in the region. These cities have high population and usually many people felt the earthquakes that occur at Badra-Amarah fault. Structures in Amara city were damaged by the mainshock of swarm of August, 2008 that has magnitude of 5.7 Mw.
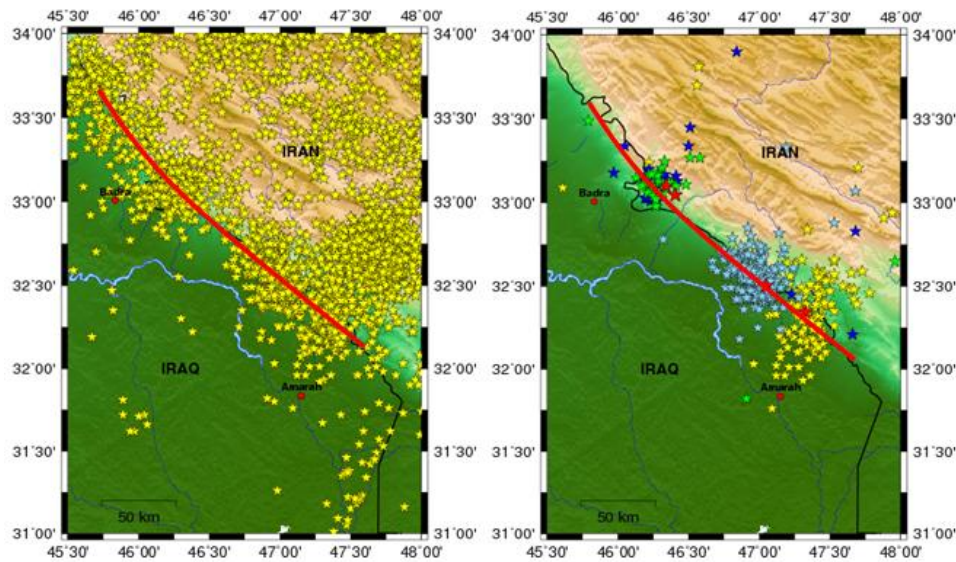


**Figure 2:** Seismicity of Badra-Amara fault area according to the (IRSC) catalog (yellow stars in the left panel) and Badra-Amarah fault (red line). The right panel represents a map showing the location of the four swarms. Yellow, green, blue, and sky blue stars are swarms 1, 2, 3, and 4 respectively. Red stars represent the mainshocks.
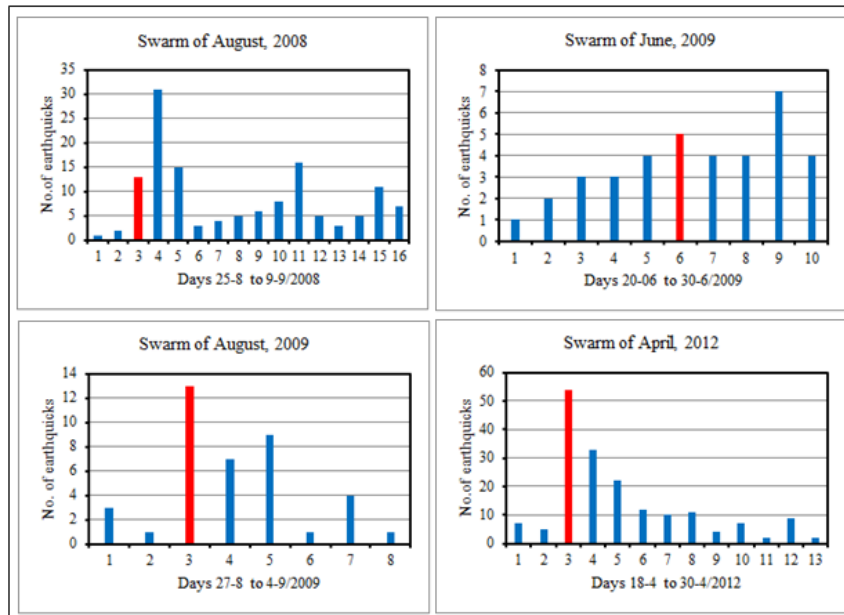


**Figure 3:** Statistical descriptions of seismic swarms along Badra-Amarah fault. Red column depicts the day of mainshock.

**Table 1:** Source parameters of the mainshocks of the four swarms along Badra-Amarah fault taken from different sources.

| Swarm | Date | Time (UTC) | Lat. | Lon. | Depth km | Mag. | Mag. Type | Source |
|---|---|---|---|---|---|---|---|---|
| August, 2008 | 2008/08/27 | 21:52:38.8 | 32.450 | 47.350 | 10.0 | 5.7 | Mw | EMSC |
| | 2008/08/27 | 21:52:40.7 | 32.344 | 47.325 | 20.5 | 5.7 | Mn | IRSC |
| June, 2009 | 2009/06/25 | 15:04:53.0 | 33.130 | 46.400 | 18.0 | 4.5 | mb | IRIS |
| | 2009/06/25 | 15:04:51.0 | 33.010 | 46.340 | 10.0 | 4.4 | mb | EMSC |
| | 2009/06/25 | 15:04:53.0 | 33.102 | 46.341 | 8.0 | 4.4 | mb | IRSC |
| August, 2009 | 2009/08/30 | 14:04:38.0 | 33.190 | 46.370 | 30.9 | 4.8 | mb | IRIS |
| | 2009/08/30 | 14:04:37.0 | 33.160 | 46.470 | 15.0 | 4.7 | mb | EMSC |
| | 2009/08/30 | 14:04:34.0 | 33.047 | 46.405 | 10.0 | 4.6 | Mn | IRSC |
| April, 2012 | 2012/04/20 | 01:21:07.0 | 32.510 | 47.020 | 10.0 | 5.1 | mb | IRIS |
| | 2012/04/20 | 01:21:10.0 | 32.530 | 47.070 | 30.0 | 5.0 | mb | EMSC |
| | 2012/04/20 | 01:21:07.3 | 32.503 | 47.049 | 20.0 | 5.1 | Mn | IRSC |

## IV. Focal Mechanism Solutions

A focal mechanism solution (FMS), or fault-plane solution, is the analysis of the fault surface on which an earthquake took place and produced seismic wave signal. From the FMS, the direction of slip and the attitude of the fault surface that caused the earthquake can be determined. Different types of focal mechanisms can be defined by beach-ball diagram. The beach-ball consists of two nodal planes, fault plane and auxiliary plane, and it is not possible to decide which nodal plane is the fault plane from only the focal mechanism beach-ball diagram, and that is called the fault plane ambiguity (Havskov and Ottemöller, 2010). The fault plane can be distinguished from the auxiliary plane based on geological field and/or remote sensing information.

One of the global institutions that are tasked to determine focal mechanism solutions for the medium to large magnitude earthquakes (mb ≥ 4.0) is the Harvard University (USA) group that estimates the Global Centroid Moment Tensor (GCMT) solutions (Dziewonski *et al*., 1981 and Ekström *et al*., 2012). Table 2 shows 18 focal mechanism solutions in the study area that were calculated from the GCMT project for the time period from 1980 to 2014. These solutions were plotted on a map as shown in Figure 4. The solutions indicate that the movements on Badra-Amarah fault is a reverse mechanisms formed by compressional forces. Only one solution out of the 18 gives a strike-slip fault mechanism which may be related with other fault with direction northeast-southwest.

**Table 2:** Source parameters and focal mechanism solutions of 18 earthquakes from the moment tensor inversion based on the GCMT project.

| No. | Date | O. Time UTC | Lat. | Lon. | D km | Mag | Mag Type | Scalar Moment dyne-cm | Plane 1 S | Plane 1 D | Plane 1 R | Plane 2 S | Plane 2 D | Plane 2 R | P PL | P AZ | N PL | N AZ | T PL | T AZ |
|---|---|---|---|---|---|---|---|---|---|---|---|---|---|---|---|---|---|---|---|---|
| 1 | 1988/01/26 | 09:34:51.1 | 32.33 | 46.85 | 19.9 | 5.5 | Mw | 2.62e+24 | 306 | 20 | 079 | 137 | 70 | 094 | 25 | 224 | 04 | 316 | 65 | 053 |
| 2 | 2001/03/23 | 05:24:15.2 | 32.78 | 46.29 | 15.0 | 5.4 | Mw | 1.45e+24 | 301 | 42 | 074 | 142 | 50 | 104 | 04 | 222 | 11 | 313 | 79 | 111 |
| 3 | 2004/10/16 | 10:04:37.6 | 33.56 | 45.63 | 14.2 | 4.8 | Mw | 2.18e+23 | 282 | 42 | 19 | 177 | 77 | 130 | 21 | 238 | 39 | 346 | 43 | 126 |
| 4 | 2005/01/25 | 11:39:20.9 | 33.40 | 45.69 | 12.0 | 4.9 | Mw | 2.97e+23 | 350 | 27 | 129 | 127 | 70 | 72 | 23 | 231 | 17 | 133 | 61 | 010 |
| 5 | 2008/08/27 | 21:52:43.4 | 32.23 | 47.36 | 12.5 | 5.8 | Mw | 5.81e+24 | 247 | 84 | -5 | 338 | 85 | -174 | 01 | 112 | 82 | 017 | 08 | 203 |
| 6 | 2008/09/03 | 22:43:16.8 | 32.44 | 47.10 | 12.0 | 5.1 | Mw | 5.7e+23 | 294 | 34 | 78 | 128 | 57 | 98 | 12 | 212 | 07 | 304 | 77 | 063 |
| 7 | 2012/02/28 | 23:18:53.5 | 32.58 | 46.81 | 12.0 | 5.0 | Mw | 3.59e+23 | 298 | 45 | 78 | 134 | 46 | 101 | 01 | 216 | 08 | 306 | 82 | 123 |
| 8 | 2012/03/08 | 18:21:38.6 | 32.79 | 46.73 | 15.6 | 5.0 | Mw | 4.28e+23 | 294 | 30 | 81 | 125 | 61 | 95 | 16 | 211 | 05 | 302 | 74 | 049 |
| 9 | 2012/03/24 | 05:25:37.2 | 32.59 | 46.84 | 12.0 | 4.9 | Mw | 2.64e+23 | 317 | 41 | 109 | 113 | 52 | 74 | 06 | 214 | 12 | 123 | 77 | 328 |
| 10 | 2012/04/18 | 18:43:00.1 | 32.54 | 46.85 | 12.0 | 5.0 | Mw | 4.05e+23 | 301 | 43 | 84 | 129 | 47 | 95 | 02 | 215 | 04 | 305 | 86 | 098 |
| 11 | 2012/04/18 | 20:04:07.9 | 32.52 | 46.93 | 12.0 | 4.9 | Mw | 2.75e+23 | 328 | 47 | 129 | 98 | 55 | 56 | 04 | 211 | 27 | 119 | 62 | 310 |
| 12 | 2012/04/20 | 01:21:08.9 | 32.53 | 46.83 | 12.0 | 5.2 | Mw | 8.13e+23 | 298 | 37 | 85 | 124 | 53 | 93 | 08 | 211 | 03 | 302 | 81 | 051 |
| 13 | 2012/04/20 | 03:05:45.3 | 32.63 | 46.73 | 12.0 | 5.2 | Mw | 8.73e+23 | 292 | 42 | 73 | 135 | 50 | 105 | 04 | 214 | 12 | 305 | 78 | 105 |
| 14 | 2012/04/20 | 03:52:37.3 | 32.61 | 46.73 | 12.5 | 4.8 | Mw | 2.19e+23 | 285 | 43 | 54 | 150 | 56 | 118 | 12 | 221 | 26 | 317 | 61 | 109 |
| 15 | 2012/04/20 | 03:56:27.9 | 32.65 | 46.58 | 12.3 | 4.9 | Mw | 2.68e+23 | 277 | 31 | 39 | 152 | 71 | 115 | 22 | 223 | 24 | 323 | 57 | 095 |
| 16 | 2012/04/20 | 15:37:06.2 | 32.62 | 46.79 | 17.9 | 4.8 | Mw | 1.80e+23 | 294 | 43 | 73 | 136 | 50 | 105 | 04 | 216 | 11 | 306 | 78 | 108 |
| 17 | 2012/04/20 | 16:17:52.2 | 32.50 | 46.90 | 12.0 | 5.0 | Mw | 4.36e+23 | 292 | 34 | 78 | 127 | 57 | 98 | 12 | 211 | 07 | 302 | 76 | 063 |
| 18 | 2012/04/21 | 05:25:11.8 | 32.45 | 46.75 | 18.9 | 5.2 | Mw | 7.53e+23 | 285 | 31 | 43 | 156 | 69 | 114 | 21 | 228 | 22 | 327 | 59 | 099 |

O. Time (UTC) origin time, Lat latitude in degree, Lon longitude in degree, D calculated depth, Mag reported magnitude, S strike, D dip, R rake angle, P, N, and T compressional, normal, and tensional moment stress axes respectively, PL plunge angle, AZ azimuth.
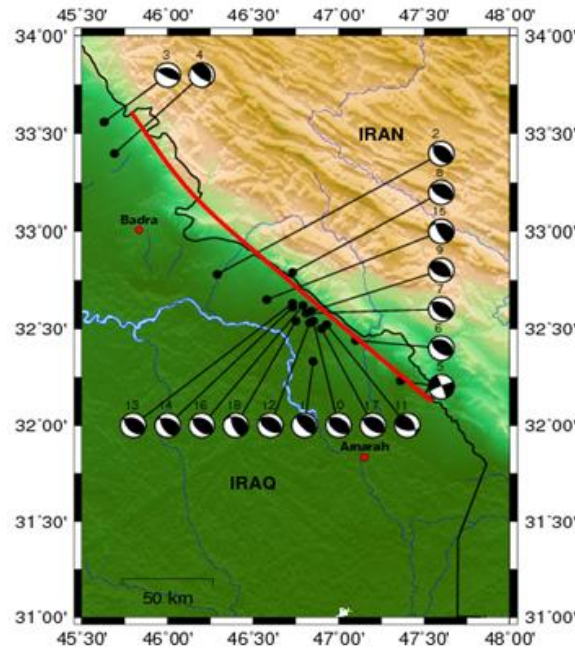
**Figure 4:** Focal mechanism solutions of 18 earthquakes in Babra-Amarah fault area from the GCMT project based on table 2.

## V. Recent Stress Analysis

From the focal mechanism solution (FMS), the direction of slip and the orientations of the moment stress axes on the fault surface during an earthquake can be determined. These axes are the maximum compressional axis (P), neutral or null axis (N or B), and maximum tensional axis (T). Dataset of the moment stress axes can be used to infer the three principal stress axes; these are the maximum stress axis $\sigma_1$, the intermediate stress axis $\sigma_2$, and the minimum stress axis $\sigma_3$. In this study, two methods of stress inversion were used to calculate the principal stress axes and stress ratio. These methods are the Improved Right Dihedron and the Rotational Optimization methods. The results of the first method have been used as a starting point for the second method.

Windows version of the TENSOR program (Win-Tensor version 4.0.4) was used to invert the moment stress axes to principal stress axes and stress ratio. This program is free source program developed originally in DOS by Delvaux (1993) and modified for Windows by Delvaux and Sperner (2003). The graphical output of the stress inversion by the TENSOR program depicts the projection of the principal stress axes in a lower hemisphere equal-area projection and allows evaluating the overall quality of the result (Delvaux and Barth, 2010). Abdulnaby *et al*. (2014) used this method to determine the stress patterns in northern Iraq and surrounding regions. In this paper they discussed the formal stress inversion methods. For more details about these methods see Abdulnaby *et al*. (2014).

Figure 5 represents the lower-hemisphere equal-area stereographic projections of the formal stress inversion of 15 focal mechanism solutions of earthquakes which occurred on Badra-Amarah fault. The left panel is the result of applying Rotational Optimization method, while right panel is the final focal mechanism of the fault. The small circle on the upper left corner of the left panel shows the direction and type of the horizontal stress axes. The histograms to the lower left corner of the stereograms depict the distribution of the misfit angle F5 in the TENSOR program weighted arithmetically according to the magnitude for each case. The stress inversions 15 focal mechanism solutions of the study area were determined to be of A quality (QRfm in the left panel of Figure 5). The right panel of Figure 5 shows the two solutions of Badra-Amarah fault which is reverse fault with a slight oblique dextral strike-slip component of the overall displacement. The fault plane solution is 60°/226° (dip angle and dip direction), while the axillary plane solution is 32°/023°. The attitudes (plunge angle and plunge direction) of the principal stress axes are: $\sigma_1=14°/217°$, $\sigma_2=10°/309°$ and $\sigma_3=72°/074°$.
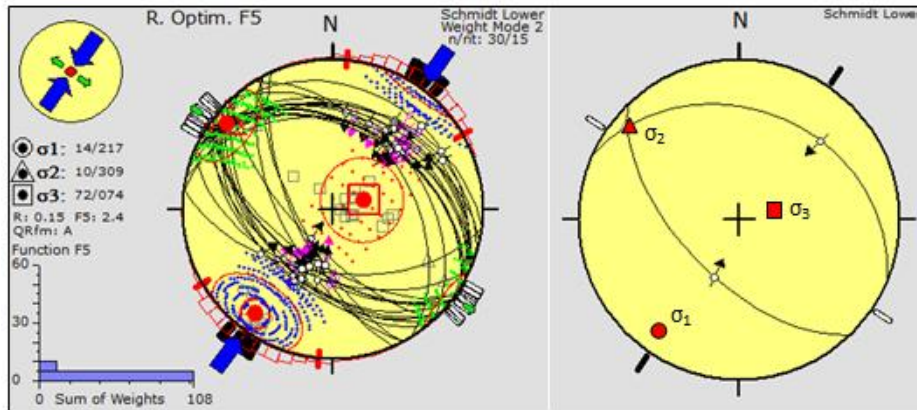
**Figure 5:** The results of formal stress inversion of 15 focal mechanism solutions by the Rotational Optimization method (left panel) and the final solution of Badra-Amarah fault (right panel). For more detail see the text.

## VI.      Results and Conclusions

Badra-Amarah fault represents the northeastern structural boundary of the Mesopotamian sagged basin. The length of fault is about 200 km and it may be extending more than that. The fault is marked by alluvial fans on the northeastern side of the Mesopotamian Zone. Seismic history during the last ten years revealed that Badrah-Amarah fault had four big swarms according to the IRSC. The mainshocks of these swarms have magnitudes ranged from 4.4 to 5.7. All these four mainshocks were happened after several foreshocks which can be used as a prediction sign.

Based on focal mechanism solutions of Badra-Amarah fault, which were collected from the GCMT project, the fault has reverse movement with a slight dextral strike-slip displacement due to compressional tectonic forces of collision zone between the Arabian and Eurasian plates. From the tectonic history of the region, Badra-Amarah fault formed as a normal fault due to the extensional forces during the Late Triassic period (Numan, 1997). The recent reverse displacement on the Badra-Amarah fault surface is due to the compressional forces that accommodate the recent tectonic movements of the Arabian and Eurasian plates. The hanging wall of the Basdra-Amarah fault is still not passing the footwall regarding the dip direction of the fault. The dip of Badra-Amarah fault is 60° with dip direction 226° (S 46° W). The attitudes of principal stress axes that are responsible for reverse movement on fault surface are: $\sigma_1=14°/217°$, $\sigma_2=10°/309°$ and $\sigma_3=72°/074°$. Figure 6 depicts simple structural model of the Mesopotamian Zone. In this model the Mesopotamian Zone is represented by a cross section of a huge graben extending from NE to SW. More seismological and structural studies are needed to provide a refined and more coherent understanding about the high seismic activity and the style of the fault.
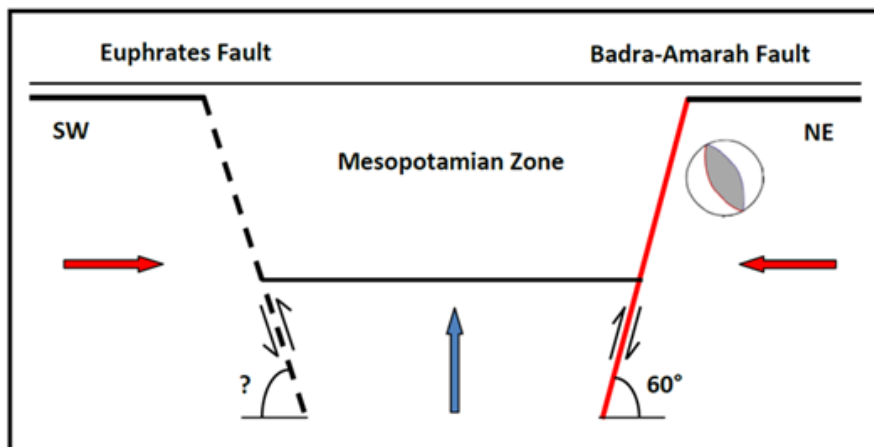


**Figure 6:** Simple structural model of the Mesopotamian Zone shows Badra-Amarah fault, Euphrates fault, and compressional stress regime in the area (without scale). Red line and broken black line represent Badra-Amarah fault and Euphrates fault respectively. The recent compressional stress regime in the study area is represented by red arrows. Blue arrow depicts the uplift in the Mesopotamian Zone caused as a secondary force by the main compressional forces.

## References

[1]. Abdulnaby, W., Mahdi, H., Al-Shukri, H., and Numan, N. M. S. (2014), Stress patterns in northern Iraq and surrounding regions from formal stress inversion of earthquake focal mechanism solutions, Pure and Applied Geophysics, 171, 2137-2153.

[2]. Delvaux, D. (1993), 'The TENSOR program for paleostress reconstruction: examples from the east African and the Baikal rift zones.' In: Terra Abstracts. Abstract supplement No. 1 to Terra Nova, 5, 216.

[3]. Delvaux, D. and Sperner, B. (2003), 'Stress tensor inversion from fault kinematic indicators and focal mechanism data: the TENSOR program.' In: *New Insights into Structural Interpretation and Modelling*, Nieuwland, D. (Ed.) Geological Society, London, Special Publications, 75-100.

[4]. Delvaux, D., and Barth, B. (2010), African stress pattern from formal inversion of focal mechanism data, Tectonophysics, 482, 105-128.

[5]. Dewey, J. F., Pitman, W. C., Ryan, W. B. F., and Bonnin, J. (1973), Plate tectonics and evolution of the Alpine system, Bull. Geol. Soc. Am., 84, 3137-3180.

[6]. Dziewonski, A. M., Chou, T. A., and Woodhouse, J. H. (1981), Determination of earthquake source parameters from waveform data for studies of global and regional seismicity, J. Geophys. Res., 86, 2825-2852.

[7]. Ekström, G., Nettles, M., and Dziewonski, A. M. (2012), The global CMT project 2004-2010: Centroid-moment tensors for 13,017 earthquakes, Phys. Earth Planet. Inter., 200-201, 1-9.

[8]. Havskov, H., and Ottemöller, L. (2010), Routine data processing in earthquake seismology, Springer, New York, 352P.

[9]. Jassim, S. Z. and Goff, J. C. (Ed.) (2006), Geology of Iraq, Dolin, Prague and Moravian Museum, Brno, Czech Republic, 486P.

[10]. Keilis-Borok, V. L., Knopoff, L., Rotwain, I. M. and Siderenko, T. M. (1978), Bursts of seismicity as long term precursors of strong earthquakes, Proc. Conf. VI, Methodology for Identifying Seismic Gaps and Soon to Break Gaps, pp. 351-386.

[11]. Michael, A. J. and Toksoz, M. N. (1982), Earthquake swarms as a long-range precursor to large earthquakes in Turkey, Geophys. J. R. astr. Soc., 68, 459-476.

[12]. Numan, N. M. S. (1997), A plate tectonic scenario for the Phanerozoic succession in Iraq, Iraqi Geological Journal, 30, 85-119.